Ocean Science

Discussions

Open Access

EGU

Pending recovery in the strength of the meridional overturning circulation at 26°N

Ben. I. Moat[1], David. A. Smeed[1], Eleanor Frajka-Williams[1], Damien G. Desbruyères[2], Claudie Beaulieu[3], William E. Johns[4], Darren Rayner[1], Alejandra Sanchez-Franks[1], Molly O. Baringer[5], Denis Volkov[5], Harry L. Bryden[6]

5 1) National Oceanography Centre, University of Southampton Waterfront Campus, European Way, Southampton, SO14 3ZH, UK.

2) Ifremer, University of Brest, CNRS, IRD, Laboratoire d'Océanographie Physique et Spatiale, IUEM, Ifremer centre de Bretagne, Plouzané, 29280, France.

3) Ocean Sciences Department, University of California Santa Cruz, CA, USA.

10 4) Rosenstiel School of Marine and Atmospheric Science, University of Miami, Miami, FL, USA.

5) Atlantic Oceanographic and Meteorological Laboratory, NOAA, Miami, FL, USA,

6) School of Ocean and Earth Science, University of Southampton Waterfront Campus, European Way, Southampton, SO14 3ZH, UK.

Correspondence to: Ben Moat (ben.moat@noc.ac.uk)

15 **Abstract.** The strength of the Atlantic meridional overturning circulation (AMOC) at 26°N has now been continuously measured by the RAPID array over the period Apr 2004 - Sept 2018. This record provides unique insight into the variability of the large-scale ocean circulation, previously only measured by sporadic snapshots of basin-wide transports from hydrographic sections. The continuous measurements have unveiled striking variability on timescales of days to a decade, driven largely by wind-forcing, contrasting with previous expectations about a slowly-varying, buoyancy forced large-scale
20 ocean circulation. However, these measurements were primarily observed during a warm state of the Atlantic Multidecadal Variability (AMV) which has been steadily declining since a peak in 2008-2010. In 2013-2015, a period of strong buoyancy-forcing by the atmosphere drove intense watermass transformation in the subpolar North Atlantic and provides a unique opportunity to investigate the response of the large-scale ocean circulation to buoyancy forcing. Modelling studies suggest that the AMOC in the subtropics responds to such events with an increase in overturning transport, after a lag of 3-9 years. At
25 45°N, observations suggest that the AMOC may already be increasing. We have therefore examined the record of transports at 26°N to see whether the AMOC in the subtropical North Atlantic is now recovering from a previously reported low period commencing in 2009. Comparing the two latitudes, the AMOC at 26°N is higher than its previous low. Extending the record at 26°N with ocean reanalysis from GloSea5, the transport fluctuations follow those at 45°N by 0-2 years, albeit with lower magnitude. Given the short span of time and anticipated delays in the signal from the subpolar to subtropical gyres, it is not
30 yet possible to determine whether the subtropical AMOC strength is recovering.

Ocean Science
Discussions
EGU
Open Access

1 Introduction

The Atlantic Meridional Overturning Circulation (AMOC) is a large-scale circulation pattern spanning the Atlantic from south to north, transporting warm waters northward and colder waters southward. It drives a large net northward transport of heat, with one petawatt (1 PW = 10^{15} W) released to the atmosphere between 26°N and 70°N, with far-reaching impacts on the

35   climate in the North Atlantic region (e.g. Srokosz et al., 2012) on surface temperatures, precipitation and sea level (Delworth and Mann, 2000). The deeper limb of the AMOC is isolated from the atmosphere and can store energy and matter for centuries. Changes to the AMOC during the paleoclimate period are thought to explain the abrupt shifts in climate found in paleoclimate records (e.g., Barber et al. 1999, Ganopolski and Rahmstorf, 2001), and the current generation of coupled climate models predicts a slowing of the AMOC over the next century in response to increasing greenhouse gases (IPCC, 2013).

40   This widespread interest in the Atlantic circulation led to the installation of the RAPID-MOCHA-WBTS array (hereafter referred to as the RAPID 26°N array) which has now been in operation, making continuous measurements of the large-scale circulation for more than 15 years (Frajka-Williams et al., 2019). Given its role in climate, the AMOC was previously thought to be slowly varying, on 'climate' timescales (decadal and longer), and so the ocean and climate communities were surprised when the first published data from RAPID 26°N demonstrated large-amplitude variability on sub-annual timescales

45   (Cunningham et al., 2007). Subsequent releases of the data, following the recovery and redeployment of instruments, yielded new insights into seasonal (Kanzow et al., 2010), interannual (McCarthy et al., 2012) and lower frequency fluctuations (Smeed et al., 2014; Smeed et al., 2018) in the basin-wide transports at 26°N. One remarkable finding from the RAPID array was the apparent dominance of wind-forcing on the annual cycle as well as the sustained dip in the AMOC strength in 2009-2010 (Roberts et al., 2013; Zhao and Johns, 2014a; Zhao and Johns, 2014b), calling into question the community's prior expectation

50   that the large-scale overturning circulation is driven by buoyancy forcing at high latitudes (Lozier 2010).
The observations to-date have occurred during a warm period of the multidecadal changes in the large-scale North Atlantic indicated by the Atlantic Multidecadal Variability (AMV, Zhang et al., 2019). While definitions for this index vary, they generally agree that the AMV was positive during a period spanning the late 1990s, peaking around 2008-2010, then a decline towards zero and even negative values depending on the definition of the AMV used (Frajka-Williams et al., 2017; Zhang et

55   al. 2019). Numerical investigations into the relationship between the AMOC and AMV demonstrate a causal link with the AMOC driving changes in the AMV, where the northward heat transport by the AMOC accumulates in North Atlantic and generates a positive ocean temperature (subsurface and surface) anomaly that is indexed by the AMV (Moat et al., 2019). The decline from a peak in 2008-2010 occurred just prior to a cold anomaly in the subpolar North Atlantic, termed the 'cold blob', and driven in large part by intense air-sea buoyancy fluxes in the winters of 2013/14 and 2014/15 (Duchez et al., 2016; Josey

60   et al., 2018). This cold anomaly heralds both a cooler state in the multidecadal variability, but also provides a large-amplitude 'impulse'-like forcing to the large-scale ocean, in a region with known sensitivity of the AMOC (Robson et al., 2014).
While the subpolar AMOC has been observed since 2014 by the OSNAP array (Lozier et al., 2019), the record is too short to document the period prior to the intense surface forcing to determine whether it is an anomalous period. However, a surface-

forced index of watermass transformation in the subpolar gyre, and a multi-dataset estimate of the AMOC at 45°N indicated
broad agreement (on timescales longer than 5-years) between the buoyancy forcing and the overturning strength (Desbruyères
et al., 2019). This record of the overturning strength indicates a strong increase in the AMOC at 45°N since about 2009.

Here we report on the latest AMOC transport time series at 26°N from April 2004 through the end of August 2018. We give
an overview of the variability of the AMOC transport using the complete record, including the seasonal cycle and interannual
variability, as well as the contributions of component parts of the circulation (Florida Current/Gulf Stream transport vs
meridional Ekman transport vs mid-ocean transports between the Bahamas and Canary Islands). We then update the findings
of Smeed et al. (2018) which reported a multiyear reduction in the AMOC strength using change point analysis. Guided by the
findings at 45°N, we then make preliminary investigations into the meridional coherence of the AMOC transport variability
between 26°N and 45°N, and the response at 26°N to the impulse forcing in 2013/15. Finally, we place the latest AMOC
transport record in context of the larger-scale Atlantic variability, its heat content and the AMV index. These latest results
show a possible recovery of the AMOC strength since its lowest point in 2009, but the short duration of the record since 2014
precludes conclusive determination of the AMOC response to buoyancy forcing at this time.

2 Data

2.1 RAPID 26°N observations and transport calculations

The array (Fig. 1) spans the middle of the North Atlantic subtropical gyre close to the latitude at which the ocean heat transport
is maximum. Here the warm northward flowing waters of the western boundary current are largely confined to the Florida
Straits with a small but highly variable part flowing east of the Bahamas in the Antilles Current. Across the rest of the section
there is a broad southward recirculation of the surface waters extending across to the coast of Africa where seasonally varying
upwelling gives rise to cooler water along the shelf edge. The deep southward flow of the AMOC is predominantly close the
western boundary and transports two distinct water masses: one centered around 1500 m depth, formed within the subpolar
gyre, and often referred to as Upper North Atlantic Deep Water (UNADW), and the other below 3000 m originating in the
Nordic Seas and referred to as Lower North Atlantic Deep Water (LNADW). Deeper still, Antarctic Bottom Water (AABW)
flows northward in the western basin.

The objective of the RAPID 26°N array is to obtain a continuous and accurate record of the AMOC volume transport, and the
associated meridional heat and freshwater transports. There are three principal components to the measurements: (1) the flow
through the Florida Straits, the Florida Current, is monitored by a subsea cable calibrated by frequent hydrographic surveys
(www.aoml.noaa.gov/phod/floridacurrent/), (2) the flow on the steep continental slope east of the Bahamas is measured by
direct velocity measurements from an array of current meters referred to as the western boundary wedge (WBW), and (3) east
of the WBW, geostrophic balance is used to estimate the flow from an array of dynamic height moorings. Instruments include,
at present, 155 CTDs (conductivity-temperature-depth), 61 current meters, 3 ADCPs (acoustic Doppler current profilers), 43
CTD-Os (CTDs with oxygen), 36 bottom pressure recorders (BPRs) and 4 PIES (pressure-inverted echo sounders). The

Ocean Science
Discussions

Open Access

dynamic height moorings are arranged in three sub-arrays: the western boundary array, the Mid-Atlantic Ridge (MAR) array and the eastern boundary array. In addition the non-geostrophic meridional Ekman transport is derived from the ERA5 reanalysis for zonal surface stress. A full description of the methodology for calculating the AMOC transports is given in McCarthy et al. (2015), and updated in the dataset release notes at https://www.rapid.ac.uk/rapidmoc/rapid_data/datadl.php.

2.2 AMOC transport at 45°N

The AMOC at 45°N has been calculated using a combination of satellite altimetry, reanalysis products and in situ ocean data (Desbruyères et al., 2019). Note, however, that the AMOC at 45°N is defined in density classes (AMOCρ). At 26°N, the transport variability is unlikely to be strongly different between the AMOC in depth-space and density-class as isopycnals across the broad expanse of the basin (6000km) are nearly flat. However, in the subpolar gyre, the overturning is defined in density coordinates (Pickart and Spall 2007; Mercier et al. 2015; Lozier et al. 2019) to better account for the dynamics of buoyancy redistribution in the ocean, which is also carried out by the horizontal gyre circulation. In the subpolar gyre, overturning is a measure of watermass transformation between net the northward 'inflow' and southward 'outflow', irrespective of the depth at which it occurs.

2.3 Other data sets

The monthly average ocean heat content was calculated using temperature profiles from the EN4 v4.2.1 gridded 1° gridded dataset (Good et al., 2013). The sea surface temperature (SST) product used here was the monthly average ERA5 reanalysis at 0.25° resolution (C3S, 2017) from 1979 to present. The winter (JFM) North Atlantic Oscillation (NAO) time series was calculated from the monthly mean NAO from the NOAA Climate prediction centre.

The AMV is a measure of the low frequency variability in the Atlantic on multidecadal timescales, calculated from sea surface temperatures (SSTs) as a North Atlantic average, with the background tendency (Enfield et al., 2001) or background field (Trenberth and Shea, 2006) removed. Here, we use the definition following Sutton and Dong (2012) which is the normalized difference between the 10-year smooth Atlantic SST (equator to 65°N, 75°W to 7.5°W) and global mean SST which is close to that of Trenberth and Shea (2006). This definition contrasts from earlier definitions which averaged the North Atlantic SSTs and then detrended over the record. However, detrending is subject to the time period under consideration and does not allow for nonlinear variations in the time series of global SSTs (Frajka-Williams et al., 2017; Zhang et al., 2019).

3 Methods

3.1 Time series processing

The Florida Current transport is produced at daily resolution after a 3-day low-pass filter is applied. Individual instrument records at 26°N are either half-hourly or hourly, and filtered with a 2-day low pass filter to remove tides. Transports are then

125 calculated on a 12-hour grid, with a 10-day low-pass filter applied. Here the data are binned to 10-day time intervals before further analysis. The seasonal cycle is calculated by least-squares fitting an annual and semi-annual harmonic, with a fixed phase and amplitude over the full (2014-2018) record. While the annual cycle appears to vary over the record, as noted in Calafat et al. (2018), further investigation of the annual cycle of transports is beyond the scope of the current investigation. Anomalies relative to the seasonal cycle are low-pass filtered using a 540-day Tukey filter.

130 Spectra are calculated using a Welch's overlapped segment averaging approach, with a Hamming taper and 50% overlap on the detrended, 10-day binned time series. In order to retain variability at low frequencies, while reducing noise at high frequencies, we 3 different window lengths following Kanzow et al., (2010).

For investigations into the relationship between the AMOC at 26°N and 45°N, we consider the geostrophic portion of the AMOC transports. i.e., at 26°N, we subtract the Ekman component from the total AMOC. This is because the Ekman
135 component is independently forced at different latitudes and would not be anticipated to show low frequency coherence between latitudes. The AMOC transport at 45°N is computed without a contribution from surface Ekman transport. Both records are then filtered with a 5-year lowpass Tukey filter.

3.2 Changepoint analysis

To analyse the variability of the AMOC transports, we use changepoint analysis on the 10-day AMOC-Ekman time series.
140 The methodology is described in Beaulieu & Killick (2018) and is similar to that used in Smeed et al. (2018). A suite of eight models were fitted to the data, in which the short term variability is modelled by either random white-noise or a first order autocorrelation [AR(1)] process. The long term variability is modelled as either a constant value, a linear trend, or one or more changepoints separating periods each linear with time. Combining all these possibilities for both the short-term and long-term variability leads to a total of eight models: (i) a constant mean with a white-noise background, 'Mean', (ii) a constant mean
145 with first-order autocorrelation 'Mean+AR(1)', (iii) a linear trend 'Trend', (iv) a linear trend with first-order autocorrelation 'Trend+AR(1)', (v) multiple changepoints in the mean with a background of white-noise 'Mean+CP', (vi) multiple changepoints in the mean with first-order autocorrelation 'Mean+AR(1)+CP', (vii) multiple changepoints in the trend with white-noise 'Trend+CP', and (viii) multiple changepoints in the trend with first order autocorrelation 'Trend+AR(1)+CP'. The changepoint analysis was conducted using the R package EnvCpt (Killick et al., 2018).

4 Methods

4.1 Characterising the variability of the AMOC at 26°N

The AMOC volume transports are given in units of Sverdrups, where $1 \, Sv = 10^6 \, m^3 \, s^{-1}$. To investigate the variability in the AMOC total and component transports, we calculate spectra (Fig. 2). We only consider fluctuations with periods longer than 20 days as the method of calculating the AMOC transport makes an assumption about the net meridional mass transport; this
155 assumption is only valid on timescales longer than about 10-days (Kanzow et al. 2007). For periods shorter than about 60 days,

Ekman transport dominates the variability; at other sub-annual periods, the variability is similar among all three components. Broad peaks in the spectra are found at both annual and semi-annual frequencies, particularly for the UMO transports, however on timescales shorter than 1 year, fluctuations in the UMO and Florida Current transports are anti-correlated (anti-correlated, Frajka-Williams et al. 2016) resulting in a reduction of power at the semi-annual frequency in the AMOC strength relative to

160   the UMO. At periods longer than a year, the AMOC variability is dominated by the UMO transport.

In view of the large and broad spectral peaks we have decomposed the time series into three parts: the seasonal cycle, an interannual signal, and the residual high frequency signal (Fig. 3). There is a substantial seasonal cycle with an amplitude of 2.0 Sv and 0.7 Sv for the annual and semi-annual harmonic, explaining 11% and 2% of the variance, respectively. The residual timeseries, likewise, retains substantial variability with a range of 23.7 Sv and a standard deviation of 3.4 Sv. The large

165   amplitude, sub-annual variability is a compelling reason why continuous, time-resolved in situ observations are required to firmly establish the mean value of the AMOC transports.

For the remainder of the paper, we focus on the low frequency (interannual) variability of the AMOC and component transports (Fig. 4). Both from the spectra and the time series in Fig. 4, it is clear that the low frequency variability in the total overturning transports is governed primarily by the mid-ocean transports, i.e., the upper mid-ocean component and the lower North Atlantic

170   Deep Water layer. This is consistent with previous investigations into the AMOC variability, which showed smaller interannual variability in the Ekman and Florida Current transports than the mid-basin (Bahamas to Canary Islands). It is interesting to note, however, that a reductions in the Ekman transport closely following the two minima in the UMO transport (2009 and 2012).

The low frequency changes in the AMOC are acyclic, and, based on data through 2012, were described using a linear trend by

175   Smeed et al. (2014). However, the tendency of the time series through 2016 was not monotonic (Smeed et al., 2018), rendering a linear trend less useful at describing the observed variability. Instead, a changepoint analysis was used to fit a model to the total AMOC transport, concluding that for the record through 2016, the total AMOC transport variations were best described by two periods with consistent mean values, separated by a single changepoint in 2008-2009 (Smeed et al., 2018). Here, we apply an updated version of the changepoint analysis to the AMOC-Ekman time series through 2018, i.e. the geostrophic

180   portion of the large-scale circulation (Fig. 5). This analysis confirms the existence of a change point, now localising it around 2009-2010, but with constant mean values before and after (Fig. 5b).

Overall, these results are consistent with the previous analyses of the low frequency variability of the AMOC transport and its component parts. However, we note from the table of annual means (Table 1), that the mean in 2017/18 (calculated over the period 1 April 2017 - 31 March 2018) was 17.8 ± 4.9 Sv (mean ± standard deviation computed on the 10-day binned time

185   series). The standard deviations are large, due to substantial sub-annual fluctuations in the AMOC strength. This is larger than the value in the year with the minimum transports (2009/10, 13.5 ± 4.4 Sv) but still smaller than the year with the maximum (2005/06, 20.9 ± 4.0 Sv). While the interannual time series appears to show a steadily, if weakly, increasing AMOC transport (Fig. 4a), this is not identified as the leading behaviour in the changepoint analysis.

6

Ocean Science
Discussions

EGU

4.2 Relationship to other latitudes

190 The 2013/14 and 2014/15 winters saw the return of deep convection in the Labrador Sea in two great impulse events (Yashayaev and Loder, 2016). Those localized deep convection events are part of wider and longer-term changes in air-sea interactions that occurred over the subpolar gyre since 2010. Those changes drove an overall intensification of the light-to-dense water mass transformation rates that sustained a delayed (5-6 years) intensification of the AMOC at the southern exit of the SPG, as found in a recent observational analysis (Desbruyères et al, 2019). Building on previous modelling studies, the

195 arrival of such a signal at subtropical latitudes can be anticipated after 3-9 years, depending on on how waves or advection mediate that response across the subpolar-subtropical boundary (Johnson and Marshall, 2002; Zhang 2007; van Sebille et al. 2011). We note here that the recent results of Zou et al. (2019) show an interesting (yet unexplained) meridional connection between the variability of UNADW in the subpolar gyre and that of LNADW in the subtropical gyre, which is in line with the LNADW-dominated decadal variability observed across the RAPID array (Fig. 4d). Based on the increase in subpolar

200 watermass transformation peaking in 2013-2015, we would anticipate a sign of the increasing subtropical AMOC would be anticipated by 2017-2023. Determining the particular timing of the adjustment would provide critical groundtruth to meridional coherence investigations.

Fig. 6a shows the 5-year low-pass filtered AMOC variations at 26°N and 45°N, where both the RAPID observations and reanalysis from the Met Office GloSea5 model are shown at 26°N. Here we use the AMOC-Ekman transports which are the

205 geostrophic part of the overturning, and the part of the signal that we would expect to show meridional coherence. The records are short, particularly the in situ observations at 26°N for the filtering applied (5-years), but both latitudes show a decrease in the AMOC-Ekman over the 2004-2011 period of more than 3 Sv (45°N) and 2 Sv (26°N). This is followed by an increase at 45°N commencing around 2010-2011. Due to the length of the filter (5-years) and the relatively short duration of the in situ 26°N observations, we use GloSea5 estimates at 26°N for a longer overlap period.

210 Comparing the AMOC-Ekman strength between 45°N and GloSea5 estimates at 26°N, we find that they show similar timing of relative peaks (1996-1997, 2004-2005) and troughs (2000-2001, 2011, 2011-2013). The AMOC-Ekman at 45°N slightly leads anomalies at 26°N (0-2 years) which is consistent with model studies that predict propagation from high to low latitudes (Zang 2010; Ortega et al., 2017). With these two time series, the variability in the GloSea5 estimate of AMOC-Ekman at 26°N is more markedly lower than at 45°N. It is worth noting again that the AMOC at 45°N is in density space, following the choice

215 in Desbruyeres et al. (2019), but that the $AMOC_z$ at 45°N is in phase with the $AMOC\rho$, but with lower amplitude (Desbruyeres et al., 2019, Figure S4). In addition, the ratio of meridional heat transport to AMOC, a measure of how 'efficient' the overturning circulation is at fluxing heat, is greater at 26°N than 45°N (Johns et al., 2011, Desbruyeres et al., 2019). This means that smaller amplitude fluctuations of the AMOC 26°N than 45°N may be associated with equivalent heat transport variability. More thorough investigations into depth- and zonal-distribution of changes at 26°N that accompany the subtle

220 intensification of the overturning strength are pending. These may enable a more conclusive determination of the arrival of the buoyancy-forced signals in the subtropical North Atlantic.

4.3 Ongoing changes in the wider Atlantic

To place the low frequency variability of the AMOC noted above in the wider Atlantic context, we consider large-scale variations in ocean heat content, SST and atmospheric variability. On the one hand, the AMOC is anticipated to respond to

225 wind- and buoyancy-forcing, and on the other, it drives heat transport and through it, heat content and SST changes.

On multidecadal timescales, Gulev et al., (2013) provided observational evidence that in the mid-latitude North Atlantic and on timescales longer than 10 years, surface turbulent heat fluxes are indeed driven by the ocean and may force the atmosphere, whereas on shorter timescales the converse is true. Numerical simulations identified a driving role in the subtropical meridional heat transport for temperature tendencies in the subpolar gyre (Moat et al., 2019). While the current record of in situ

230 observations is too short to fully-investigate multi-decadal relationships, we can look more closely at the period of the observations and the longer records of ocean heat content and SSTs to evaluate whether the observed variations in the Atlantic, as indexed by the AMV, follow the patterns predicted by the numerical simulations.

The AMV is a record of the multidecadal variations in the North Atlantic, based on SST (Fig. 6b). Since 1985, there was a steady increase in North Atlantic SSTs, peaking in 2008 followed by a decline. The full-depth ocean heat content (OHC)

235 anomaly in the subpolar North Atlantic (80°W to 20°E, 45°N to 67°N) shows a similar pattern of change, indicating that while the AMV is a record of SSTs, it is indicative of subsurface temperatures as well. From e.g., Moat et al. (2019) in a 1/4 degree ocean model, we anticipate that changes in the AMOC lead the AMV by about 4 years. The North Atlantic Oscillation index (NAO) is an indicator of the atmospheric state. The lowpassed NAO was in a positive state with a maximum in 1991 and declining to near zero in 2011. It is out-of-phase with the AMV and ocean heat content. The relationship between NAO, AMOC

240 at 26°N, AMV and ocean heat content is consistent with the pattern described in Sutton et al. (2018).

Comparing the large-scale climate indices with the transport estimates at two latitudes, we can evaluate the relationship between heat transported by the ocean and the temperature changes in the Atlantic. After the NAO maximum around 1990, the AMOC reaches a peak (around 1996 at 45°N and 1997 in the GloSea5 estimate (Jackson et al., 2019)), followed by an increase in the AMV to a maximum in 2007, and a high anomaly in full depth ocean heat content between 2006-2012, with a

245 peak in 2012. As the AMOC transports decreased, relative to these previous strong values, the heat they transport northward decreases proportionally (Johns et al., 2011). During the low AMOC period around 2010, both 26°N and 45°N fluxed less heat northwards. All else being the same (no changes in surface fluxes or transports across the Greenland-Iceland-Scotland (GIS) ridge), this weak AMOC state is likely to explain the observed cooling of the subpolar North Atlantic. While the heat transport and transport variability across the GIS ridge are small (Østerhus et al., 2019), the surface fluxes during this period did change

250 notably during the 2013-15 cold anomaly in the subpolar North Atlantic (Duchez et al., 2016, Josey et al. 2018). A more complete diagnosis of the heat budget, and the relative contributions of ocean transports and surface fluxes, is beyond the scope of this paper. We note, however, that the extended AMOC time series at 45°N, and the reanalysis estimates from GloSea5 at 26°N (Jackson et al., 2019) indicate a phased relationship between the AMOC and AMV that is consistent with a role for the ocean in driving changes in North Atlantic climate.

Ocean Science
Discussions

Open Access

5 Conclusions

From the nearly 15-year long record of the AMOC variability at 26°N, we can characterise the transports as highly variable on all timescales, with high frequency variability dominated by rapid fluctuations in the zonal winds across 26°N, seasonal cycles contributed by the UMO transport between the Bahamas and Canary Islands, and low frequency variability dominated by the UMO transports and mirrored in the Lower North Atlantic Deep Water layer (3000-5000m). This is in agreement with previous investigations into the seasonal cycle (Kanzow et al. 2010, Duchez et al. 2014), high frequency variability (Moat et al. 2016) and compensation between components (Kanzow et al. 2007, Frajka-Williams et al. 2016), and interannual and longer term variability (McCarthy et al. 2012, Smeed et al. 2014, Smeed et al. 2018). One remarkable finding from these previous studies was the apparent dominance of wind-forcing on the annual cycle as well as the sustained dip in the AMOC strength in 2009-10 (Roberts et al. 2013), calling into question the community's prior expectation that the large-scale overturning circulation is driven by buoyancy forcing at high latitudes (Lozier 2010). Observations from a range of latitudes in the Atlantic confirmed that the presence of high frequency fluctuations is ubiquitous, from the South Atlantic (34.5°S) to the subpolar North Atlantic (Frajka-Willams et al. 2019).

The recent intense heat loss in the subpolar North Atlantic (2013-2015) and the extension of the RAPID record through 2018, motivated an investigation into whether and when the RAPID transports would respond to buoyancy forcing in the subpolar gyre forcing. In situ estimates of the overturning at 45°N indicate that at this latitude, near the southern boundary of the subpolar gyre, the overturning strength is already intensifying following sustained buoyancy forcing in the subpolar gyre (Desbruyères et al. 2019). Comparing the transport variability at 26°N and 45°N, we show some indication of a potential lead-lag relationship (45°N leading changes at 26°N by 0-2 years) in the AMOC-Ekman transports, but with stronger amplitude variations at 45°N. Given that the results at 45°N follow the basin-wide surface-forced transformation in the subpolar gyre by 5 years, and the 0-2 years further lag to 26°N, we would anticipate an intensification in the overturning strength at 26°N in response to the 2013-15 forcing by 2019-2021. The length of the records collected to date are somewhat short, given the smoothing applied (5 years), and so determination of a lead-lag relationship through lagged correlation cannot provide significance. Instead, we have relied on a more speculative identification of peaks and troughs in the time series.

In addition to the AMOC at 26°N responding to subpolar changes, the heat transport variability at 26°N, particularly on longer timescales, is anticipated to lead to changes in the subpolar North Atlantic and broader Atlantic as a whole. The phase-relationship identified in the modelling study of Moat et al. (2019) relies on identifying periods where the AMOC is increasing or decreasing, or where it is positive vs negative (corresponding to increasing or decreasing accumulated northward heat transport). With the record at hand, it is difficult to determine a 'reference period' around which to define an anomaly. Instead we note that the phased relationship with high values of the AMOC strength at 26°N (GloSea5 reanalysis) and 45°N occur during a period when the AMV is increasing (North Atlantic is warming), while the change in tendency of the AMV occurs when the AMOC values are low.

The transport time series at 26°N in the Atlantic of the large-scale ocean circulation has yielded new insights into the variability of the overturning circulation (Srokosz and Bryden, 2015). The results here extend our understanding of the AMOC variability through 2018 and investigate whether the recent strong buoyancy forcing in the subpolar gyre (2013-2015) is apparent yet in the transports at 26°N. We have concluded that the AMOC appears to be marginally stronger in the period 2014-2018 than the preceding period (2009-2014) and that this increase began roughly 0-2 years following the observed increase at 45°N. While the in situ record at 26°N is too short to conclusively determine the lag, a comparison between model reanalysis (GloSea5) AMOC at 26°N and the AMOC at 45°N supports this timing. Using these longer records, we find that the changes in the AMOC strength are consistent with an ocean role in driving variations in North Atlantic temperatures, but a more complete heat budget analysis is under investigation for a conclusive determination of the relative importance of ocean transports vs surface forcing.

Data availability

The RAPID-MOCHA-WBTS time series (Smeed et al., 2019) is available at http://www.rapid.ac.uk/rapidmoc. ERA5 sea surface temperature (SST) is available via https://www.ecmwf.int/en/forecasts/datasets/reanalysis-datasets/era5. The EN4 profiles used to calculate the ocean heat content are available via https://www.metoffice.gov.uk/hadobs/en4/download-en4-2-1.html. The GloSea5 time series is available from (Jackson et al., 2019). The 45°N time series of Desbruyères et al., (2019) is available from the author on request.

Author Contributions

EFW, DAS, BIM, CB, DD wrote the manuscript with input from all authors. BIM, DR, DD, DAS, HLB contributed to the transport calculations. DAS, CB, BIM, EFW, ASF performed the analysis. WEJ, DV, MOB, BIM, DAS, DR, EFW, HLB contributed to the data collection.

Competing interests

The authors declare they have no conflict of interest.

Acknowledgements

Ocean Science
Discussions

315 **References**

Barber, D. C., Dyke, A., Hillaire-Marcel, C., Jennings, A. E., Andrews, J. T., Kerwin, M. W., Bilodeau, F., McNeely, R., Southon, J., Morehead, M. D. and Gagnon, J.-M.: Forcing of the cold event of 8,200 years ago by catastrophic drainage of Laurentide lakes, Nature, 400:344-348, DOI:10.1038/22504, 1999.

Beaulieu, C. and Killick, R.: Distinguishing trends and shifts from memory in climate data Distinguishing trends and shifts

320 from memory in climate data, J. of Climate, 31:9519-9543. DOI:10.1175/jcli-d-17-0863.1, 2018.

Calafat F. M., Wahl, T., Lindsten, F., Williams, J. and Frajka-Williams, E.: Coherent modulation of the sea-level annual cycle in the United States by Atlantic Rossby waves, Nat. Comm., 9:2571, DOI:10.1038/s41467-018-04898-y, 2018.

Copernicus Climate Change Service (C3S) (2017): ERA5: Fifth generation of ECMWF atmospheric reanalyses of the global climate. Copernicus Climate Change Service Climate Data Store (CDS), 2019.

325 Cunningham, S. A., Kanzow T. O., Rayner D., Barringer M. O., Johns W. E., Marotzke J., Longworth H. R., Grant E. M., Hirschi J. J.-M. , Beal L. M., Meinen C. S. and Bryden H. L.: Temporal variability of the Atlantic Meridional Overturning Circulation at 26.5°N, Science, 317:935-938, DOI:10.1126/science.1141304, 2007.

Delworth, T. L. and Mann, M. E.: Observed and simulated multidecadal variability in the Northern Hemisphere, Clim. Dyn., 16, 661–676, DOI:10.1007/s003820000075, 2000.

330 Desbruyères, D. G., Mercier, H., Maze, G. and Daniault, N.: Surface predictor of overturning circulation and heat content change in the subpolar North Atlantic, Ocean Science, 15, 809–817, DOI:10.5194/os-15-809-2019, 2019.

Duchez, A., Frajka-Williams, E., Castro, N., Hirschi, J. and Coward, A.: Seasonal to interannual variability in density around the Canary Islands and their influence on the Atlantic meridional overturning circulation at 26°N, J. of Geophys. Res.: Oceans, 119:1843-1860, DOI:10.1002/2013JC009416, 2014.

335 Duchez, A., Frajka-Williams, E., Josey, S. A., Evans, D. G., Grist, J. P., Marsh, R., McCarthy, G. D., Sinha, B., Berry, D. I. and Hirschi, J. J.-M.: Drivers of exceptionally cold North Atlantic Ocean temperatures and their link to the 2015 European heat wave, Environ. Res. Lett., 11, DOI: 10.1088/1748-9326/11/7/074004, 2016.

Enfield, D. B., Mestas-Nunez, A. M. and Trimble, P. J.: The Atlantic Multidecadal Oscillation and its relationship to rainfall and river flows in the continental U.S., Geophys. Res. Lett., 28:2077–2080, DOI:10.1029/2000GL012745, 2001.

340 Frajka-Williams, E., Meinen, C.S., Johns, W.E., Smeed, D.A., Duchez, A., Lawrence, A.J., Cuthbertson, D.A., McCarthy, G.D., Bryden, H.L., Baringer, M.O., Moat, B.I. and Rayner, D.: Compensation between meridional flow components of the Atlantic MOC at 26°N, Ocean Science, 12:481-493, DOI:10.5194/os-12-481-2016, 2016.

Frajka-Williams, E., Beaulieu, C. and Duchez, A.: Emerging negative Atlantic Multidecadal Oscillation in spite of warm subtropics, Scientific Reports, 7:11224, DOI:10.1038/s41598-017-11046-x, 2017.

345   Frajka-Williams, E., Ansorge, I. J., Baehr, J., Bryden, H. L., Chidichimo, M. P., Cunningham, S. A., Danabasoglu, G., Dong, S., Donohue, K. A., Elipot, S., Heimbach, P., Holliday, N. P., Hummels, R., Jackson, L. C., Karstensen, J., Lankhorst, M., Bras, I. A. L., Lozier, M. S., McDonagh, E. L., Meinen, C. S., Mercier, H., Moat, B. I., Perez, R. C., Piecuch, C. G., Rhein, M., Srokosz, M. A., Trenberth, K. E., Bacon, S., Forget, G., Goni, G., Kieke, D., Koelling, J., Lamont, T., McCarthy, G. D., Mertens, C., Send, U., Smeed, D. A., Speich, S., van den Berg, M., Volkov, D. and Wilson, C.: OceanObs19: Atlantic

350   meridional overturning circulation: Observed transports and variability, Frontiers in Marine Science, 6:260, DOI:10.3389/fmars.2019.00260, 2019. Ganopolski, A. and Rahmstorf, S.: Rapid changes of glacial climate simulated in a coupled climate model, Nature, 409:153–158, DOI:10.1038/35051500, 2001.

Good, S. A., Martin, M. J. and Rayner, N. A.: EN4: quality controlled ocean temperature and salinity profiles and monthly objective analyses with uncertainty estimates, J. of Geophys. Res.: Oceans, 118:6704-6716, DOI:10.1002/2013JC009067,

355   2013.

Gulev, S.K., Latif M., Keenlyside N., Park, W. and Koltermann, K. P.: North Atlantic Ocean control on surface heat flux on multidecadal timescales, Nature, 499:464–467, DOI:10.1038/nature12268, 2013.

IPCC: Observations: Ocean, in: Climate Change 2013: The Physical Science Basis. Contribution of Working Group I to the Fifth Assess- ment Report of the Intergovernmental Panel on Climate Change, edited by Stocker, T. F., Qin, D., Plattner, G.-

360   K., Tignor, M., Allen, S., Boschung, J., Nauels, A., Xia, Y., Bex, V., and Midgley, P., p. 1535pp, Cambridge University Press, Cambridge, United Kingdom, DOI:10.1017/CBO9781107415324, 2013.

Jackson J. C., Dubois C., Forget G., Haines K., Harrison M., Iovino D., Kohl A., Mignac D., Mashina S., Peterson K. A., Piecuch C. G., Roberts C., Robson J., Storto A., Toyoda T., Valdivieso M., Wilson C., Wang Y. and Zuo, H.: The mean state and variability of the north Atlantic circulation: a perspective from ocean reanalyses, J. of Geophys. Res.: Oceans, 134,

365   DOI:10.1029/2019JC015210, 2019.

Johns W. E., Baringer, M. O., Beal, L. M., Cunningham, S. A., Kanzow, T., Bryden, H. L., Hirschi, J. J-M., Marotzke, J., Meinen, C. S., Shaw, B. and Curry, R.: Continuous, Array-Based Estimates of Atlantic Ocean Heat Transport at 26.5°N, J. Climate, 24:2429-2449, DOI: 10.1175/2010JCLI3997.1, 2011.

Johnson. H. L. and Marshall. D. P.: A theory for the surface Atlantic response to thermohaline variability, J. Phys. Oceanogr.,

370   32:1121-1132, DOI: 10.1175/1520-0485(2002)032<1121:ATFTSA>2.0.CO;2, 2002.

Josey S A., Hirschi, J J.-M., Sinha, B., Duchez, A., Grist, J. P. and Marsh, R.: The Recent Atlantic Cold Anomaly: Causes, Consequences, and Related Phenomena, Ann. Rev. Mar. Sci., 10, 475-501, DOI:10.1146/annurev-marine-121916-063102, 2018.

Kanzow, T., Cunningham, S. A., Rayner, D., Hirschi, J. J.-M., Johns, W. E., Baringer, M. O., Bryden, H. L., Beal, L. M.,

375   Meinen, C. S. and Marotzke, J.: Observed flow compensation associated with the MOC at 26.5°N in the Atlantic, Science, 317:938-941, DOI:10.1126/science.1141293, 2007.

Ocean Science
Discussions

Kanzow, T., Cunningham, S. A., Johns, W. E., Hirschi, J. J.-M., Marotzke, J., Baringer, M. O., Meinen, C. S., Chidichimo, M. P., Atkinson, C., Beal, L. M., Bryden, H. L. and Collins, J.: Seasonal variability of the Atlantic meridional overturning circulation at 26.5°N, J. Climate, 23:5678–5698, DOI:10.1175/2010JCLI3389.1, 2010.

380 Killick, R., Beaulieu, C., Taylor, S. and Hullait, H.: Envcpt: Detection of structural changes in climate and environment time series (Version version 1.1.1). CRAN. Retrieved from https://CRAN.R-project.org/package=EnvCpt, 2018.

Lozier, M.S.: Deconstructing the Conveyor Belt, Science, 328:1507-1511, DOI:10.1126/science.1189250, 2010.

Lozier, M. S., Li, F., Bacon, S., Bahr, F., Bower, A. S., Cunningham, S. A., de Jong, M. F., de Steur, L., de Young, B., Fischer, J., Gary, S. F., Greenan, B. J. W., Holliday, N. P., Houk, A., Houpert, L., Inall, M. E., Johns, W. E., Johnson, H. L., Johnson,

385 C., Karstensen, J., Koman, G., Le Bras, I. A., Lin, X., Mackay, N., Marshall, D. P., Mercier, H., Oltmanns, M., Pickart, R. S., Ramsey, A. L., Rayner, D., Straneo, F., Thierry, V., Torres, D. J., Williams, R. G., Wilson, C., Yang, J., Yashayaev, I. and Zhao, J.: A Sea change in our view of overturning in the subpolar North Atlantic, Science, 363:516–521, DOI:10.1126/science.aau6592, 2019.

Mercier, H., Lherminier, P., Sarajanov, A., Gaillard, F., Daniault, N., Desbruyères, D. G., Falina, A., Ferron, B., Gourcuff, C.,

390 Huck, T. and Thierry, V.: Variability of the meridional circulation at the Greenland-Portugal OVIDE section from 1993 to 2010, Prog. in Oceanogr., 132:250-261, DOI:10.1016/j.pocean.2013.11.001, 2015.

McCarthy, G., Frajka-Williams, E., Johns, W. E., Baringer, M. O., Meinen, C. S., Bryden, H. L., Rayner, D., Duchez, A., Roberts, C. D. and Cunningham, S. A.: Observed Interannual Variability of the Atlantic Meridional Overturning Circulation at 26.5°N, Geophys. Res. Lett., 39:L19609. https://doi.org/10.1029/2012GL052933, 2012.

395 McCarthy, G. D., Smeed, D. A., Johns, W. E., Frajka-Williams, E., Moat, B. I., Rayner, D., Baringer, M. O., Meinen, C. S. and Bryden, H. L.: Measuring the Atlantic meridional overturning circulation at 26°N, Prog. in Oceanogr., 130:91–111, DOI:10.1016/j.pocean.2014.10.006, 2015.

Moat, B. I., Josey, S. A., Sinha, B., Blaker, A. T., Smeed, D. A., McCarthy, G., Johns, W. E., Hirschi, J. J.-M., Frajka-Williams, E., Rayner, D., Duchez, A. and Coward, A.C.: Major variations in subtropical North Atlantic heat transport at short (5 day)

400 timescales and their causes, J. of Geophy. Res.: Oceans, 121(5):3237-3249, DOI:10.1002/2016JC011660, 2016.

Moat, B. I., Sinha, B., Josey, S. A., Robson, J., Ortega, P., Sévellec, F., Holliday, N. P., McCarthy, G. D., New, A. L. and Hirschi, J. J.-M.: Insights into decadal North Atlantic sea surface temperature and ocean heat content variability from an eddy-permitting coupled climate model, J. of Climate, 32(18):6137-6161, DOI:10.1175/JCLI-D-18-0709.1, 2019.

Ortega, P., Robson, J., Sutton, R.T. and Andrews M. B.: Mechanisms of decadal variability in the Labrador Sea and the wider

405 North Atlantic in a high-resolution climate model, Clim. Dyn., 49:2625, DOI:10.1007/s00382-016-3467-y, 2017.

Østerhus, S., Woodgate, R., Valdimarsson, H., Turrell, B., de Steur, L., Quadfasel, D., Olsen, S. M., Moritz, M., Lee, C. M., Larsen, K. M., Jónsson, S., Johnson, C., Jochumsen, K., Hansen, B., Curry, B., Cunningham, S. and Berx B.: Arctic Mediterranean exchanges: a consistent volume budget and trends in transports from two decades of observations, Ocean Science, 15:379-399, DOI:10.5194/os-15-379-2019, 2019.

Ocean Science
Discussions
Open Access
EGU

410 Pickart, R. S. and Spall, M. A.: Impact of Labrador Sea convection on the North Atlantic Meridional Overturning circulation, J. of Physical Oceanogr., 37:2207-2227, DOI:10.1175/JPO3178.1, 2007.

Roberts, C. D., Waters, J., Peterson, K. A., Palmer, M., McCarthy, G. D., Frajka-Williams, E., Haines, K., Lea, D. J., Martin, M. J., Storkey, D., Blockley, E. W. and Zuo, H.: Atmosphere drives observed interannual variability of the Atlantic meridional overturning circulation at 26.5°N, Geophys. Res. Lett., 40:5164-5170, DOI: 10.1002/grl.50930, 2013.

415 Robson, J., Sutton, R. and Smith, D.: Atlantic overturning in decline?, Nat. Geosci., 7:2-3, DOI:10.1038/ngeo2050, 2014.

Smeed, D. A., McCarthy, G., Cunningham, S. A., Frajka-Williams, E., Rayner, D., Johns, W. E., Meinen, C. S., Baringer, M.O., Moat, B. I., Duchez, A. and Bryden, H. L.: Observed decline of the Atlantic Meridional Overturning Circulation 2004–2012, Ocean Science, 10:29-38, https://doi.org/10.5194/os-10-29-2014, 2014.

Smeed, D. A., Josey, S., Johns, W., Moat, B., Frajka-Williams, E., Rayner, D., Meinen, C., Baringer, M., Bryden, H. and 420 McCarthy, G.: The North Atlantic Ocean is in a state of reduced overturning, Geophys. Res. Lett., 45:1527–1533, DOI:10.1002/2017GL076350, 2018.

Smeed D., Moat B. I., Rayner D., Johns W. E., Baringer M. O., Volkov D. L. and Frajka-Williams, E.: Atlantic meridional overturning circulation observed by the RAPID-MOCHA-WBTS (RAPID-Meridional Overturning Circulation and Heatflux Array-Western Boundary Time Series) array at 26°N from 2004 to 2018. British Oceanographic Data Centre, National 425 Oceanography Centre, NERC, UK. doi:10/c72s, 2019.

Srokosz, M., Baringer, M., Bryden, H., Cunningham, S., Delworth, T., Lozier, S., Marotzke, J. and Sutton, R.: Past, present and future changes in the Atlantic meridional overturning circulation, Bull. Amer. Meteorol. Soc., 93:1663–1676. DOI:10.1175/BAMS-D-11-00151.1, 2012.

Srokosz, M. A. and Bryden, H. L.: Observing the Atlantic Meridional Overturning Circulation yields a decade of inevitable 430 surprises, Science, 348, DOI:10.1126/science.1255575, 2015.

Sutton, R. T., McCarthy, G. D., Robson, J., Sinha, B., Archibald, A. and Gray, L.J.: Atlantic multi-decadal variability and the UK ACSIS programme. Bull. Amer. Meteorol. Soc., 99:415–425, DOI:10.1175/BAMS-D-16-0266.1, 2018.

Trenberth, K. E. and Shea, D. J.: Atlantic hurricanes and natural variability in 2005, Geophys. Res. Lett., 33:L12704, DOI:10.1029/2006GL026894, 2006.

435 Sutton, R. T. and Dong, B.: Atlantic Ocean influence on a shift in European climate in the 1990s, Nature Geosci., 5:788–792, DOI:10.1038/ngeo1595, 2012.

van Sebille, E., Baringer, M. O., Johns, W. E., Meinen, C. S., Beal, L. M., de Jong, M. F. and van Aken, H. M.: Propagation pathways of classical Labrador Sea water from its source region to 26°N, J. of Geophys. Res.: Oceans, 116:C12027, DOI:10.1029/2011JC007171, 2011.

440 Yashayaev, I. and Loder, J. W.: Further intensification of deep convection in the Labrador Sea in 2016, Geophys. Res. Lett., 44:1429–1438, DOI:10.1002/2016GL071668, 2016.

Zhang, R.: Anticorrelated multidecadal variations between surface and subsurface tropical North Atlantic, Geophys. Res. Lett., 34:L12713, DOI:10.1029/2007GL030225, 2007.

Ocean Science
Discussions

EGU

Zhang, R.: Latitudinal dependence of Atlantic meridional overturning circulation variations, Geophys. Res. Lett., 37:L16703,
445 DOI:10.1029/2010GL044474, 2010.

Zhang, R., Sutton, R., Danabasoglu, G., Kwon, Y.-O., Marsh, R., Yeager, S. G., Amrhein, D. E. and Little, C. M.: A review
of the role of the Atlantic meridional overturning circulation in Atlantic Multidecadal Variability and associated climate
impacts, Rev. of Geophys., 57:316–375, DOI:10.1029/2019RG000644, 2019.

Zhao, J. and Johns, W. E.: Wind-driven seasonal cycle of the Atlantic meridional overturning circulation, J. Phys. Oceanogr.,
450 44:1541–1562, DOI: 10.1175/JPO-D-13-0144.1, 2014a.

Zhao, J. and Johns, W. E.: Wind-forced interannual variability of the Atlantic meridional overturning circulation at 26.5°N, J.
Geophys. Res.-Oceans, 119:2403–2419, DOI: 10.1002/2013JC009407, 2014b.

Zou, S., Lozier, M. S. and Buckley, M.: How Is Meridional Coherence Maintained in the Lower Limb of the Atlantic
Meridional Overturning Circulation?, Geophys. Res. Lett., 46:244-252, DOI:10.1029/2018GL080958, 2019.

455

460

465

470

475

480

	MOC (Sv)	Ekman (Sv)	Florida Current (Sv)	UMO (Sv)
2004/05	18.4 ± 4.7	3.9 ± 3.7	32.0 ± 3.0	-17.5 ± 2.6
2005/06	20.9 ± 4.0	4.4 ± 2.5	32.0 ± 2.4	-15.5 ± 2.6
2006/07	20.3 ± 3.3	5.1 ± 2.9	31.6 ± 1.9	-16.3 ± 2.8
2007/08	18.9 ± 3.5	4.9 ± 2.7	31.7 ± 2.4	-17.6 ± 2.6
2008/09	18.0 ± 3.4	5.3 ± 2.8	31.6 ± 3.6	-18.7 ± 3.8
2009/10	13.5 ± 4.4	3.1 ± 3.9	30.7 ± 2.5	-20.2 ± 2.5
2010/11	17.4 ± 4.0	4.1 ± 3.4	31.1 ± 2.9	-17.6 ± 3.7
2011/12	18.0 ± 2.9	5.8 ± 2.6	31.1 ± 2.3	-18.7 ± 2.9
2012/13	14.8 ± 4.4	3.8 ± 3.5	30.8 ± 3.0	-19.6 ± 2.8
2013/14	18.0 ± 3.0	5.7 ± 2.6	31.5 ± 2.9	-19.0 ± 3.3
2014/15	17.2 ± 2.9	5.1 ± 2.6	30.4 ± 2.6	-18.2 ± 2.5
2015/16	17.5 ± 3.6	4.7 ± 2.8	31.6 ± 3.0	-18.8 ± 3.3
2016/17	18.0 ± 3.7	5.0 ± 2.7	32.4 ± 3.6	-19.4 ± 3.9
2017/18	17.8 ± 4.9	5.1 ± 3.7	30.7 ± 2.3	-17.9 ± 3.1

Table 1. The annual means of the MOC volume transport and components in Sverdrups (1 Sv = 1e6 m^3/s). Values are given as the annual mean ± the standard deviation of the 10-day binned values for that year. Annual means are computed from 1 April through 31 March. Positive values indicate northward transport, while negative values are southward.
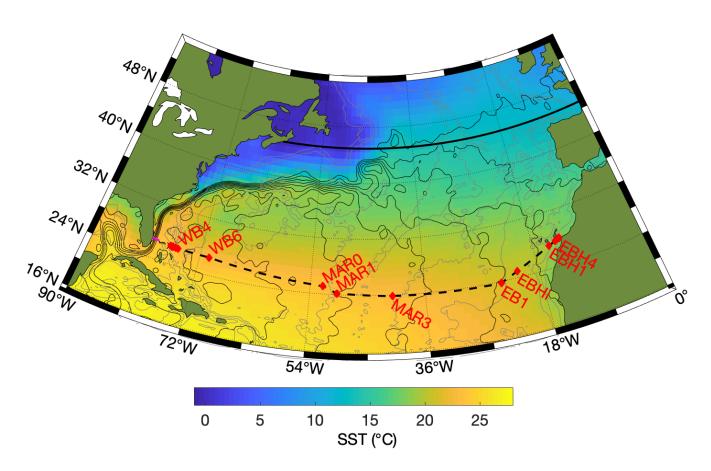
485

Figure 1 The RAPID 26°N array traverses the subtropical gyre of the North Atlantic. The magenta line shows the location of the subsea cable in the Florida Strait and red diamonds connected by a dashed black line show the location of moorings. 'WB', 'MAR', and 'EB' denote, respectively, moorings in the western boundary, mid-Atlantic Ridge and eastern boundary sub-arrays. For clarity, not all moorings are labelled. The colour shows mean sea surface temperature (SST) in March (average of 1999 to 2018) and the continuous black lines are the corresponding contours of sea surface height (contour interval 0.1m). Contours of water depth at 1000, 3000 and 5000 m are shown in grey. The thick black line at 45°N indicates where multiple data sources have been used to estimate the AMOC at the boundary between the subtropical and subpolar gyres (Desbruyères et al., 2019).
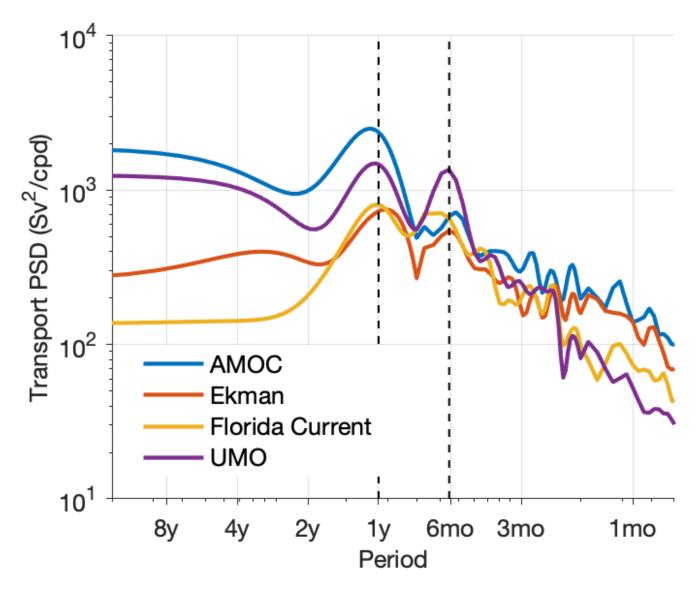
Ocean Science
Discussions

Open Access

EGU

Figure 2 Power spectral density of the AMOC and its component parts as a function of period. The vertical dashed lines highlight the annual and semiannual frequencies.
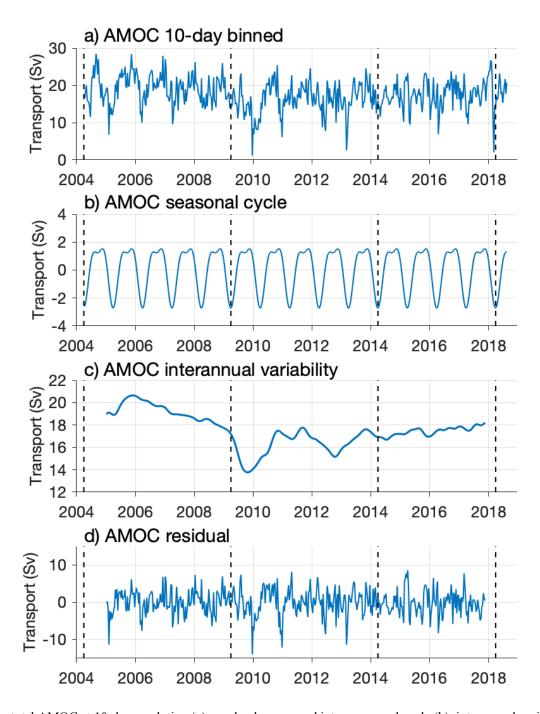
Figure 3 The total AMOC at 10-day resolution (a), can be decomposed into a seasonal cycle (b), interannual variability (c), and a residual (d). The interannual component is obtained by filtering the data with a 540-day low-pass filter after removal of
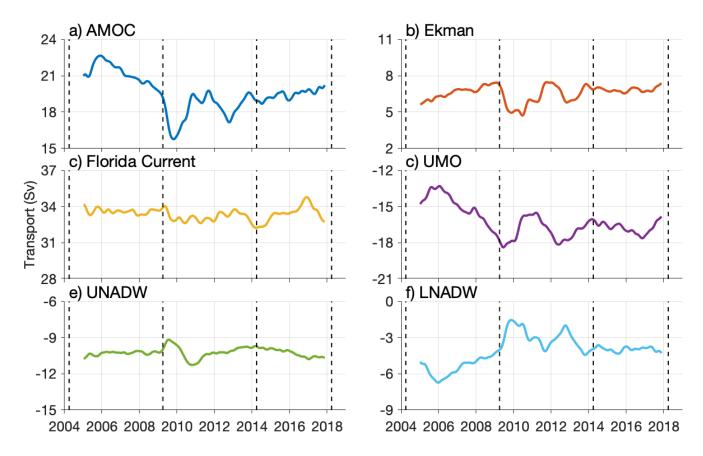505   the mean seasonal cycle.

Figure 4 Interannual variability of the AMOC at 26°N and its component parts: (a) AMOC, (b) Ekman, (c) Florida Current,
510 (d) Upper mid-ocean, (e) Upper North Atlantic Deep Water, and (f) Lower North Atlantic Deep Water.

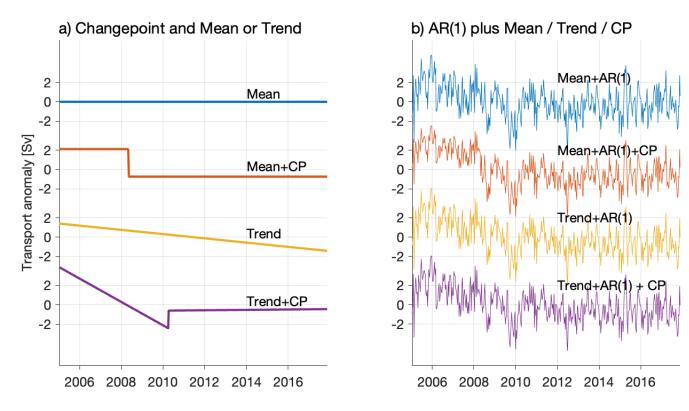Ocean Science
Discussions
Open Access

Figure 5 Changepoint analysis of the AMOC-Ekman time series. In panel (a), only a mean or a trend, with or without a changepoint are fit. In panel (b), an AR(1) is also fit. The model with the best overall fit is the Mean + AR(1) + CP model (red, right), indicating that the time series can best be explained by an AR(1) time series with a change in the mean in 2009.
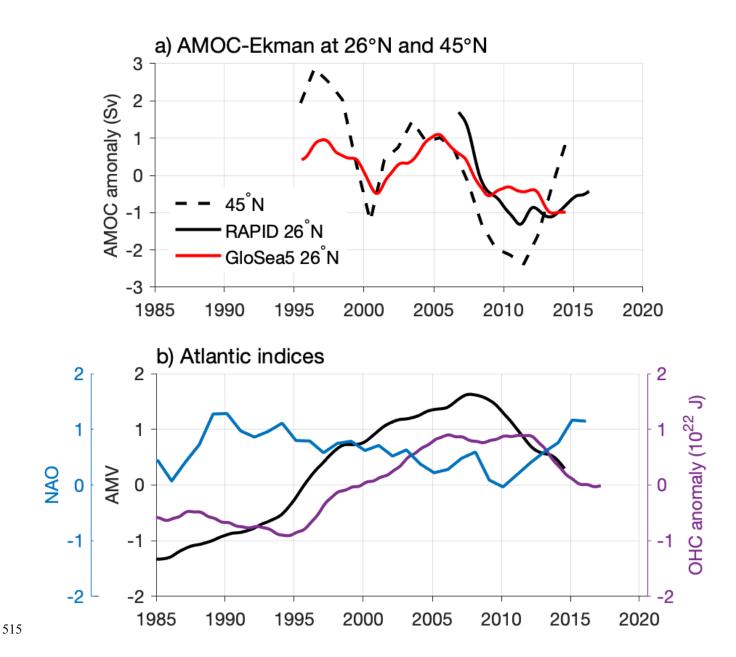
515

Figure 6 (a) AMOC anomalies from RAPID at 26°N (black, Sv), 26°N GloSea5 reanalysis (red, Sv), AMOC 45°N (black dashed, Sv). b) The AMV (black), NAO (blue) and subpolar North Atlantic (80°W to 20°E, 45°N to 67°N) full depth ocean heat content anomaly (purple, 10^{22} J). The AMV has been decadally low-pass filtered, with a 5-year low-pass filter applied to the other time series. The Ekman transport has been removed from the AMOC time series.

520